Supplementary file

Changes in drought features at European level over the last 120 years

Monica Ionita[1*] and Viorica Nagavciuc[1,2]

[1] Alfred Wegner Institute Helmholtz Center for Polar and Marine Research, Bremerhaven, Germany

[2] Forest Biometrics Laboratory – Faculty of Forestry, "Stefan cel Mare" University of Suceava, Suceava, Romania

[*] Corresponding author: Monica Ionita (Monica.Ionita@awi.de)

To analyzed if there are significant changes in the SPIE12, SPI12, scPDSI (Figure1 and Figure S2), PP, TT and PET (Figure S3) and the drought area (Figures 3 - 5) we have used the rank-based non-parametric Mann-Kendall (M-K) test and Spearman's Rho (Mann, 1945; Kendall, 1948), which are less sensitive to outliers than parametric statistics, were used. To avoid the influence of serial persistence on M-K test results, the modified M-K (MMK) trend test was used, using the computation algorithm discussed by Hamed and Rao (1998).

Table S1. Linear trends of the drought area for different drought types (moderate, severe and extreme) for SPEI12, SPI12 and scPDSI for the three analyzed regions: MED, CEU and NEU.

	SPEI12			**SPI12**			**scPDSI**		
	Moderate[i)]	Severe[ii)]	Extreme[iii)]	Moderate[i)]	Severe[ii)]	Extreme[iii)]	Moderate[i)]	Severe[ii)]	Extreme[iii)]
MED	↑*	↑*	↑*	↑	↑	↑	↑*	↑*	↑*
CEU	↑*	↑*	↑*	↓	↓	↓	↑*	↑*	↑*
NEU	↓*	↓*	↓	↓*	↓*	↓*	↓*	↓*	↓*

↑* - indicates a significant positive trend (99% significance level);
↑ - indicates a positive, but not significant trend;
↓*- indicates a significant negative trend (99% significance level);
↓ - indicates a negative, but not significant trend;

i) moderate drought (SPI/SPEI values between -1 and -1.5 and scPDSI values between -2 and -3);
ii) severe drought (SPI/SPEI values between -1.5 and -2 and scPDSI values between -3 and -4);
iii) extreme drought (SPI/SPEI values less than -2 and scPDSI values smaller than -4).

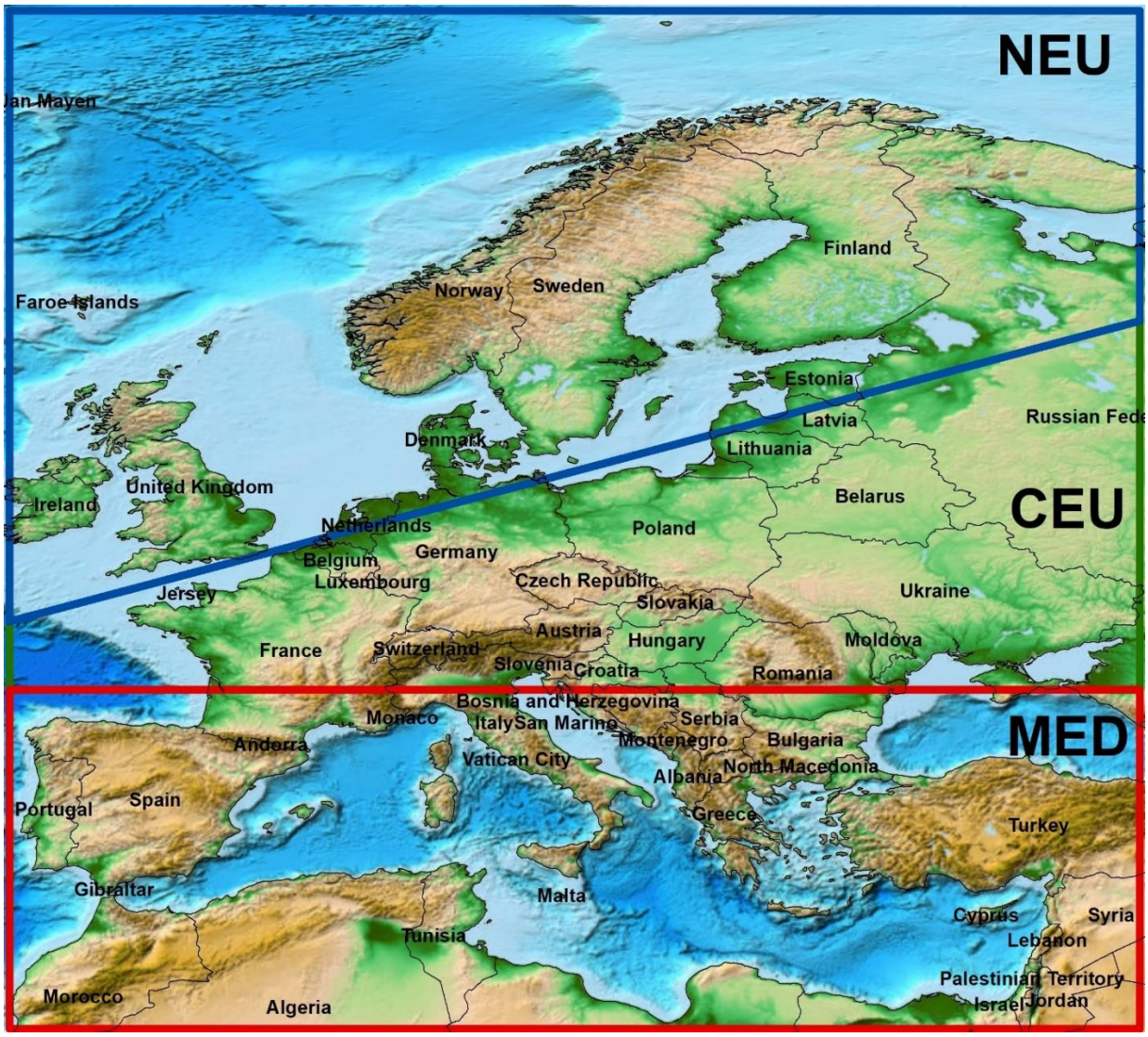

Figure S1. Spatial delimitation of the macro regions analyzed in this study: South Europe/ Mediterranean region (MED); Central Europe (CEU) and North Europe (NEU). Data source for the digital elevation model: (NOAA, 2009).

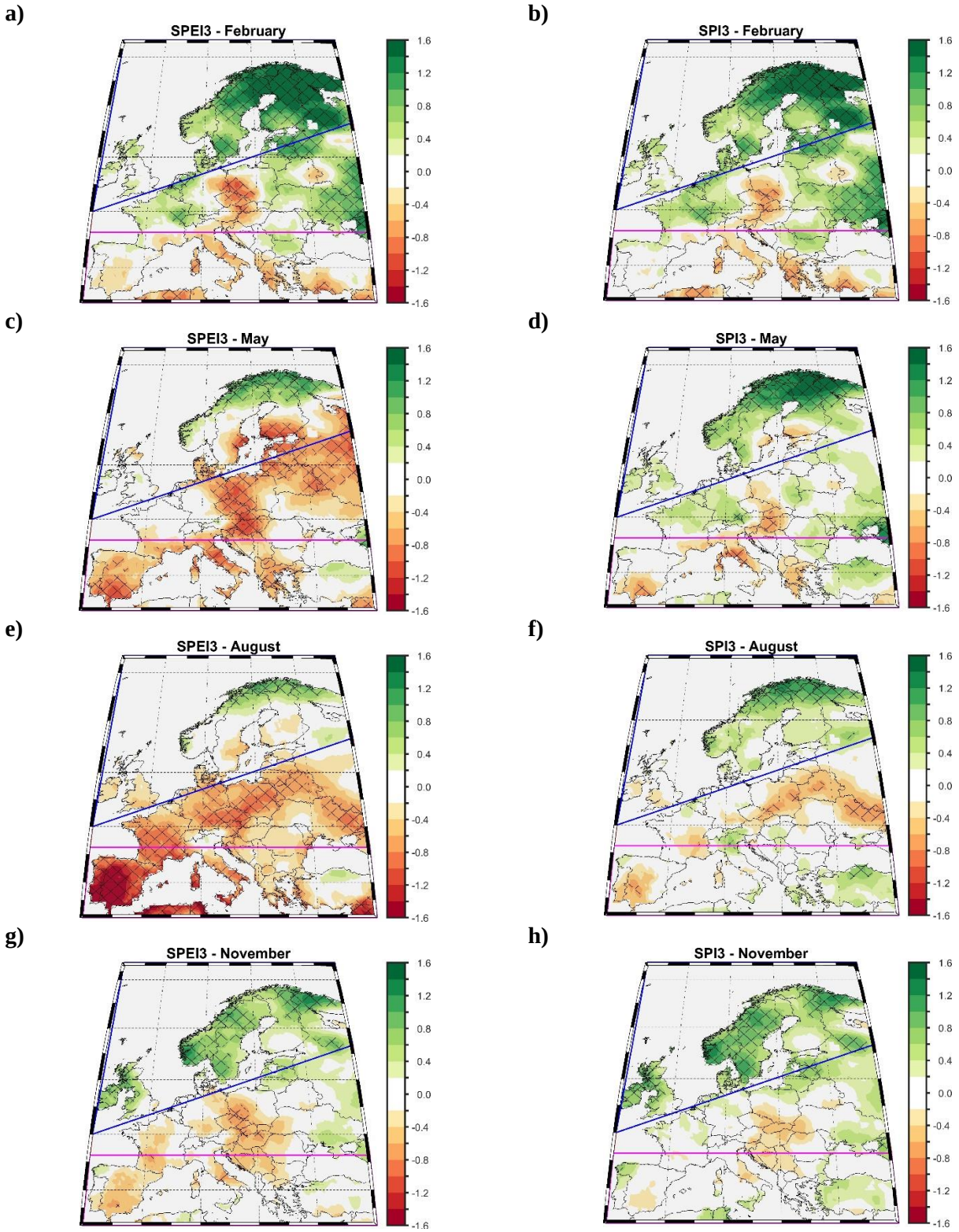

Figure S2. a) Linear trend of February SPEI3; b) as in a) but for SPI3; c) linear trend of May SPEI3; d) as in c) but for SPI3; e) linear trend of August SPEI3; f) as in e) but for SPI3; g) linear trend of SPEI3 November and h) as in g) but for SPI3. Stipples indicate statistically significant trends. Analyzed period 1902 – 2019. Units: z-scores/ 118 years.

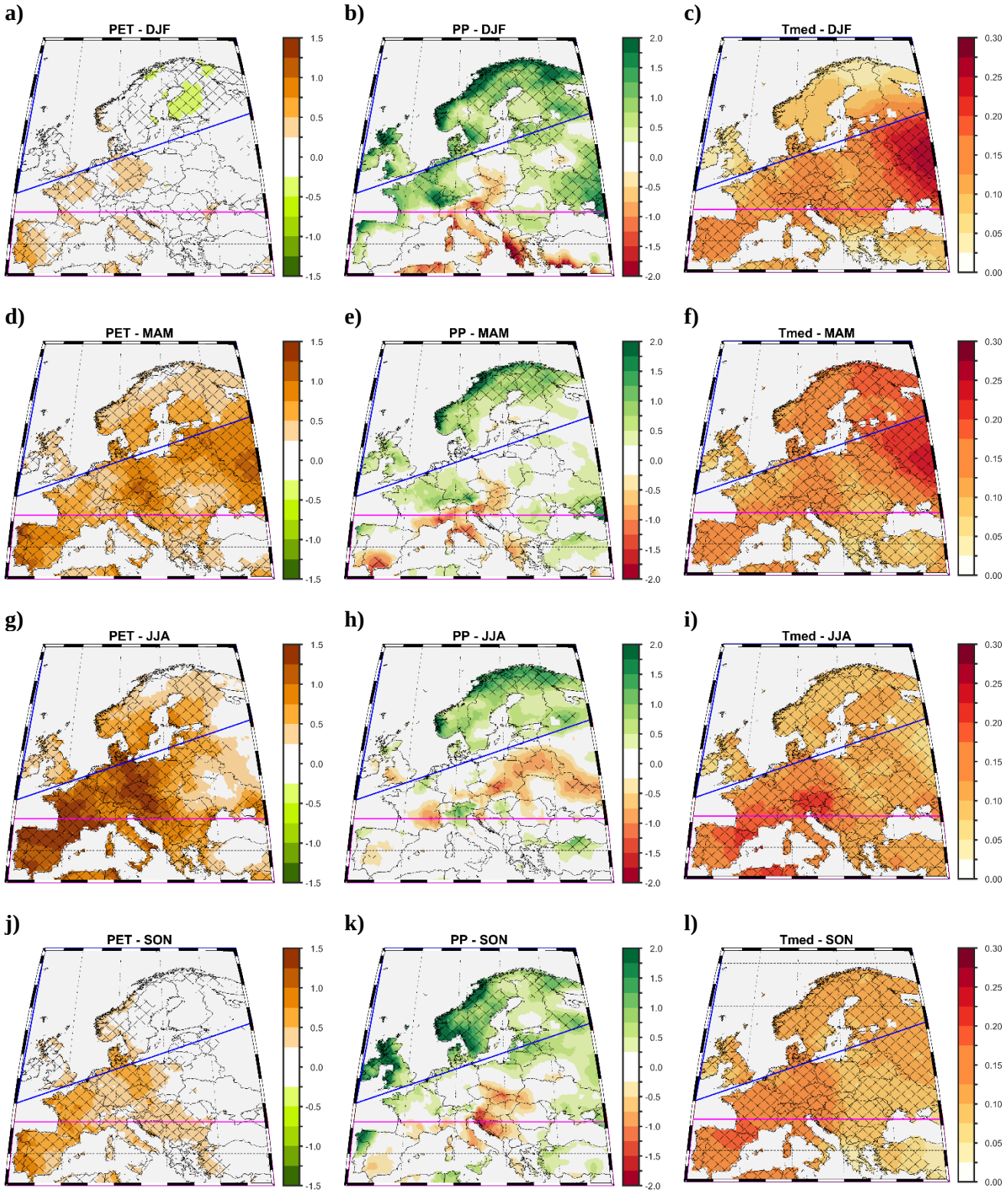

Figure S3. a) Linear trend of winter (DJF) potential evapotranspiration (PET); b) as in a) but for the winter (DJF) precipitation (PP); c) as in a) but for the winter (DJF) mean air temperature (TT); d) as in a) but for spring (MAM); e) as in b) but for spring (MAM); f) as in c) but for spring (MAM); g) as in a) but for summer (JJA); h) as in b) but for summer (JJA); i) as in c) but for summer (JJA); j) as in a) but for autumn (SON); k) as in b) but for autumn (SON) and l) as in c) but for autumn (SON). Stipples indicate statistically significant trends. Analyzed period 1902 – 2019. Units: PET (mm/decade), PP (mm/decade) and TT (°C/decade).

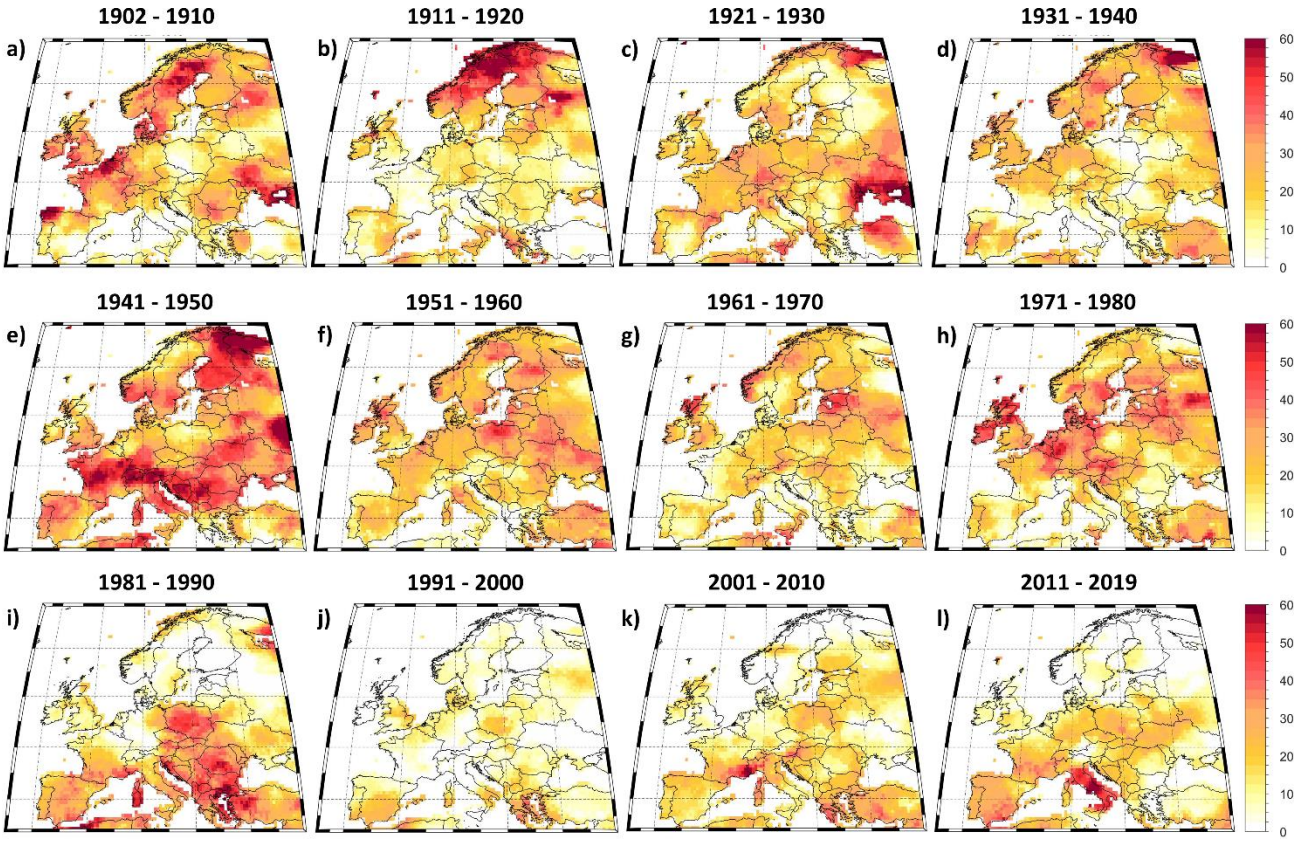

Figure S4. Decadal frequency of drought duration for **moderate drought** (SPI12 between -1.0 and -1.5): a) 1902 – 1901; b) 1911 – 1920; c) 1921 – 1930; d) 1931 – 1940; e) 1941 – 1950; f) 1951 – 1960; g) 1961 – 1970; h) 1971 – 1980; i) 1981 – 1990; j) 1991 – 2000; k) 2001 – 2010 and l) 2011 – 2019. Units: number of months/period.

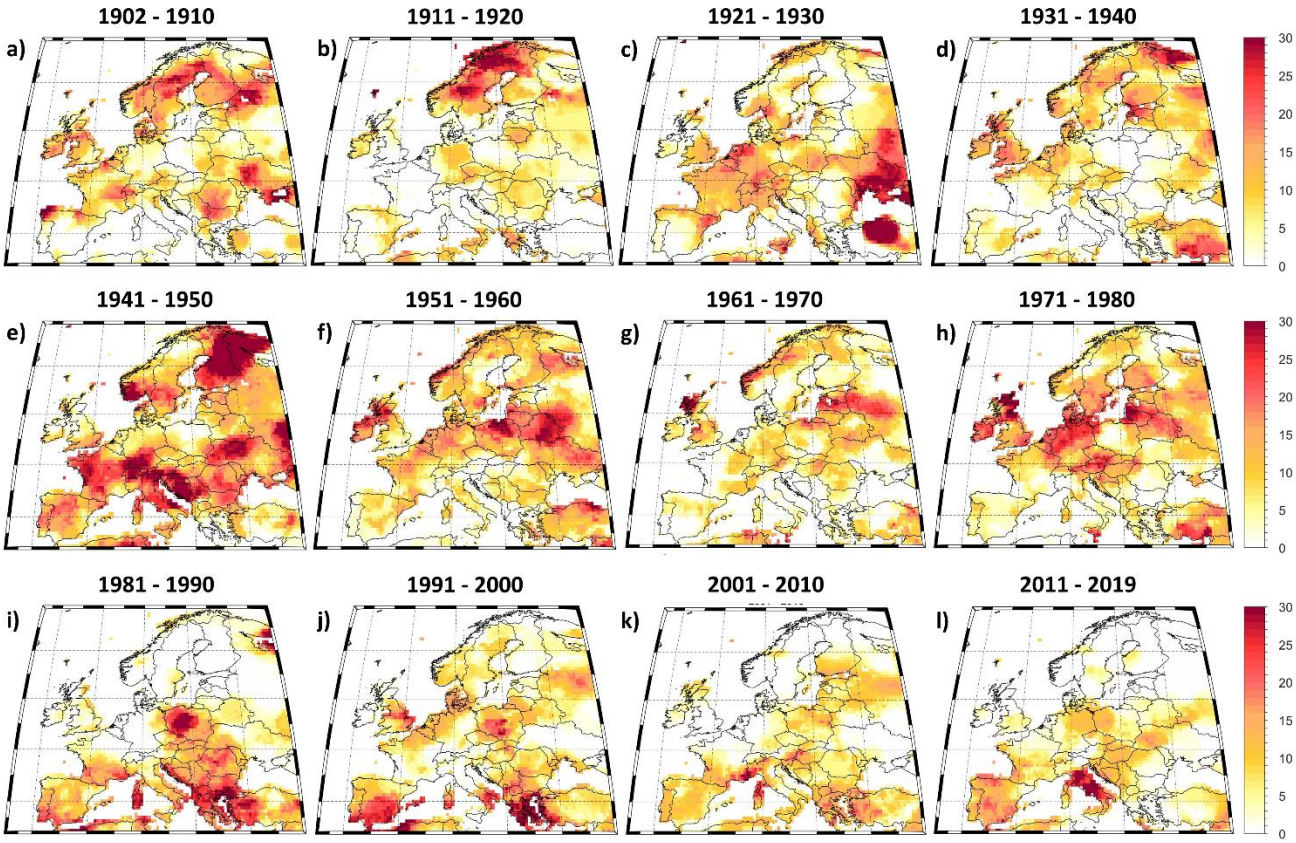

Figure S5. Decadal frequency of drought duration for **severe drought** (SPI12 between -1.51 and -2): a) 1902 – 1901; b) 1911 – 1920; c) 1921 – 1930; d) 1931 – 1940; e) 1941 – 1950; f) 1951 – 1960; g) 1961 – 1970; h) 1971 – 1980; i) 1981 – 1990; j) 1991 – 2000; k) 2001 – 2010 and l) 2011 – 2019. Units: number of months/period.

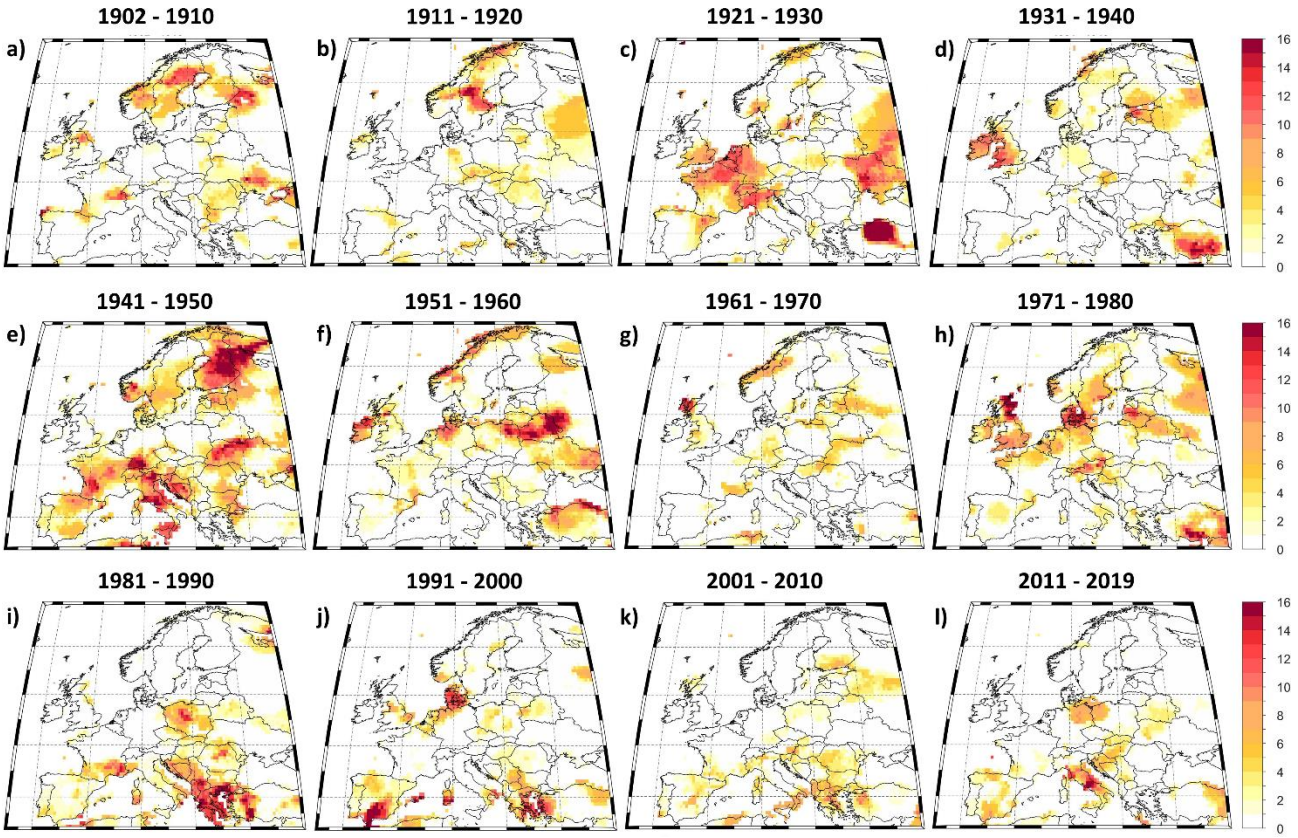

Figure S6. Decadal frequency of drought duration for **extreme drought** (SPI12<-2): a) 1902 – 1901; b) 1911 – 1920; c) 1921 – 1930; d) 1931 – 1940; e) 1941 – 1950; f) 1951 – 1960; g) 1961 – 1970; h) 1971 – 1980; i) 1981 – 1990; j) 1991 – 2000; k) 2001 – 2010 and l) 2011 – 2019. Units: number of months/period.

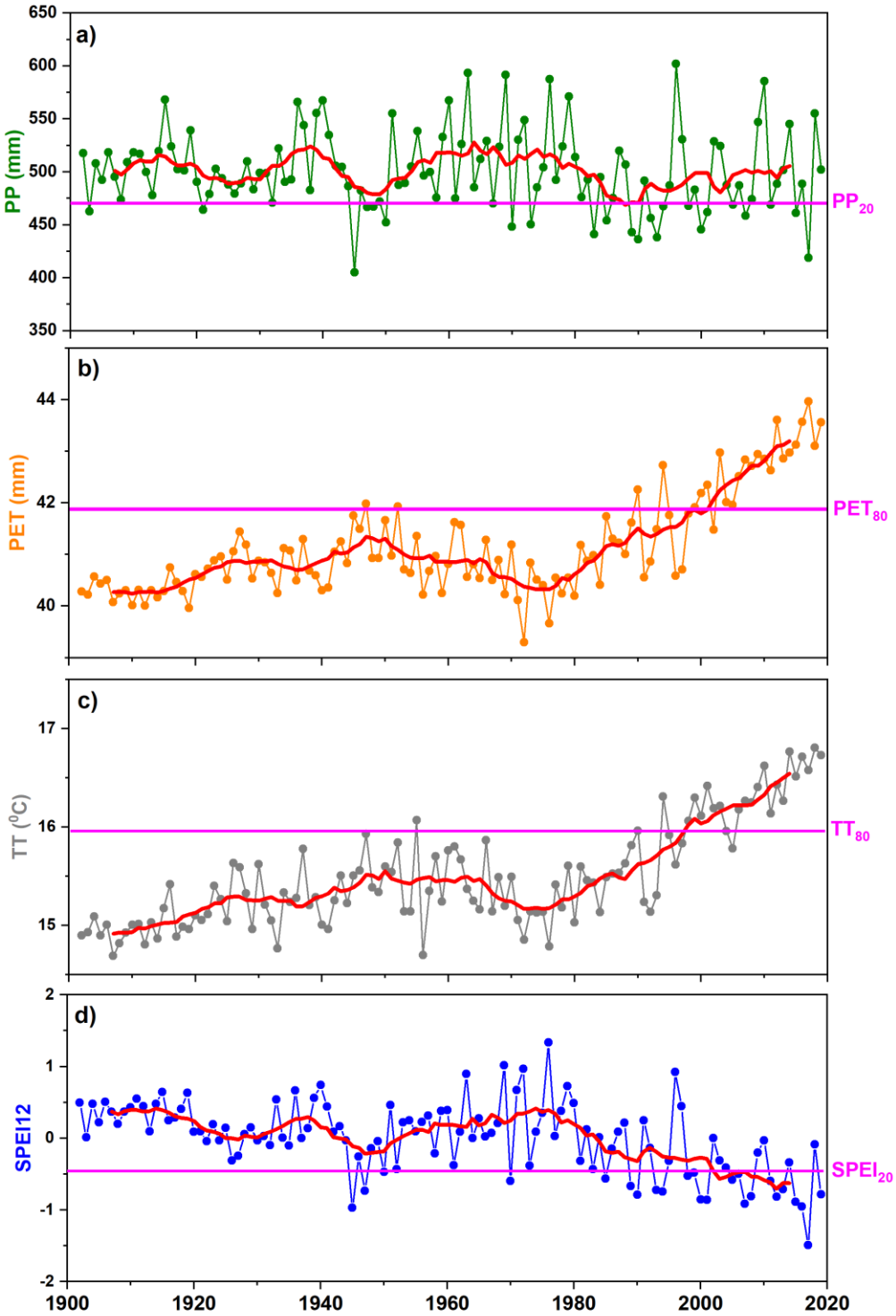

Figure S7. a) Time series of the annual precipitation (PP) averaged over MED; b) as in a) but for the potential evapotranspiration (PET); c) as in a) but for mean air temperature (TT) and d) as in a) but for SPEI12. The red line in a) – d) indicates the 21 years running mean.

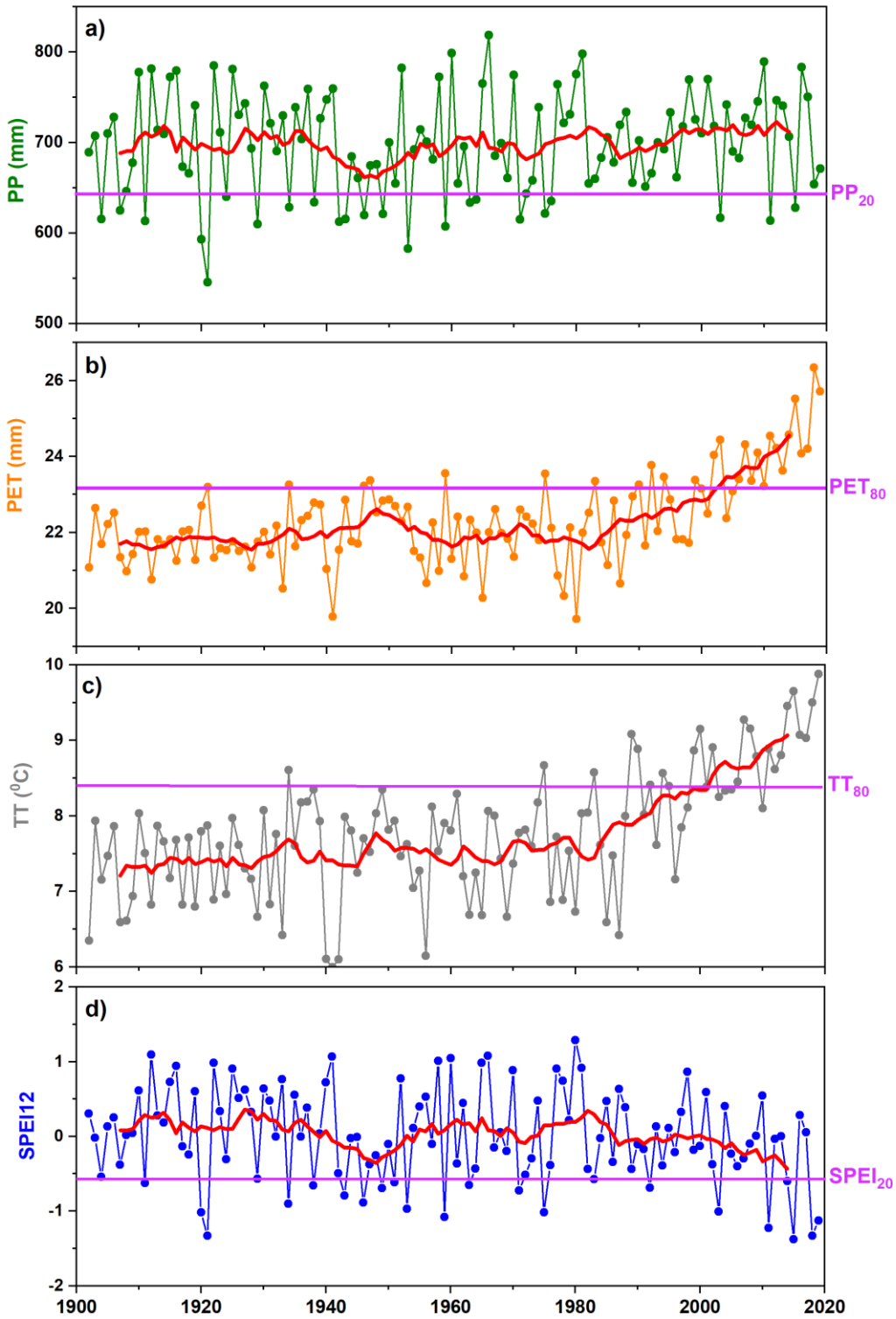

Figure S8. a) Time series of the annual precipitation (PP) averaged over CEU; b) as in a) but for the potential evapotranspiration (PET); c) as in a) but for mean air temperature (TT) and d) as in a) but for SPEI12. The red line in a) – d) indicates the 21 years running mean.

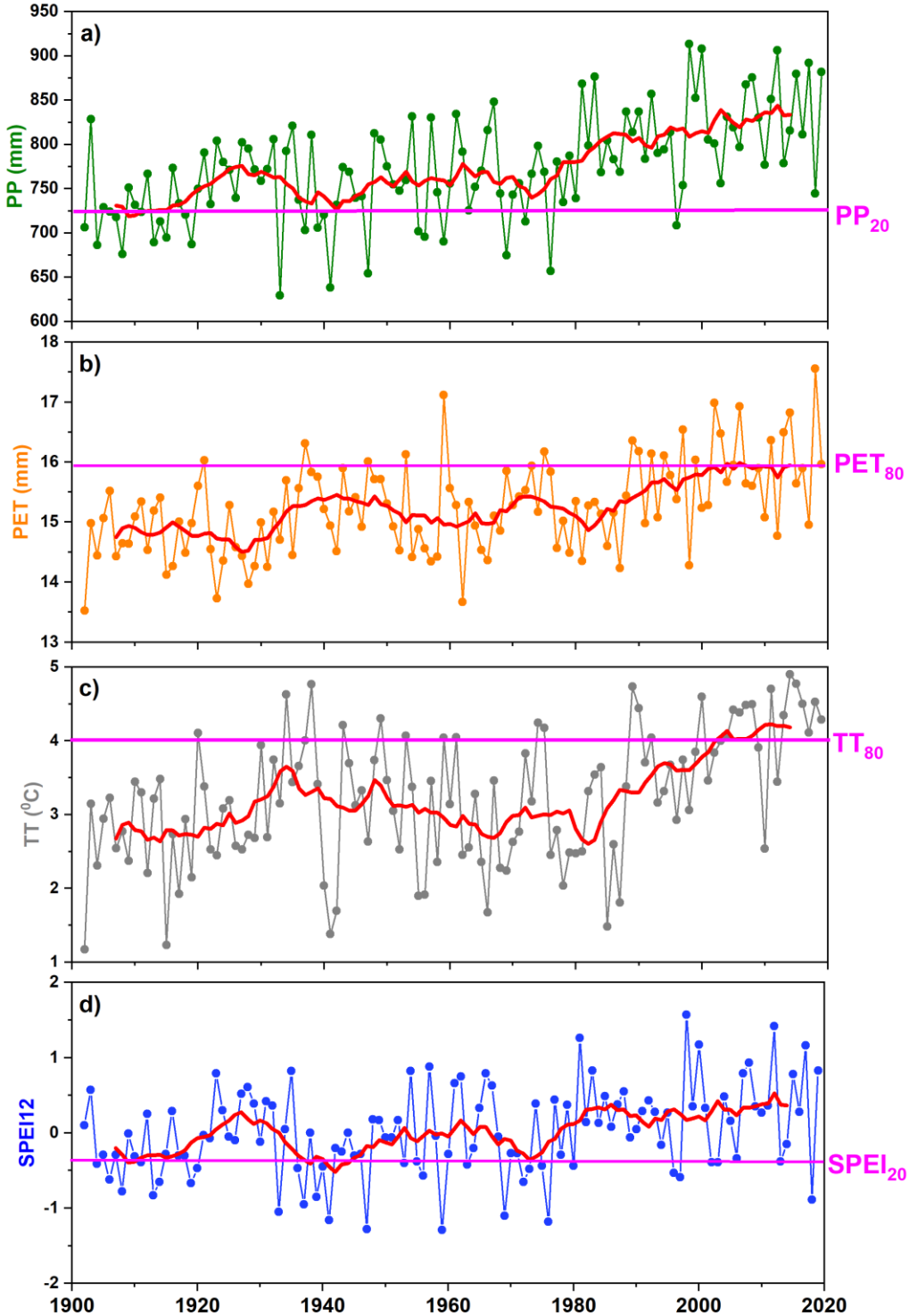

Figure S9. a) Time series of the annual precipitation (PP) averaged over MED; b) as in a) but for the potential evapotranspiration (PET); c) as in a) but for mean air temperature (TT) and d) as in a) but for SPEI12. The red line in a) – d) indicates the 21 years running mean.

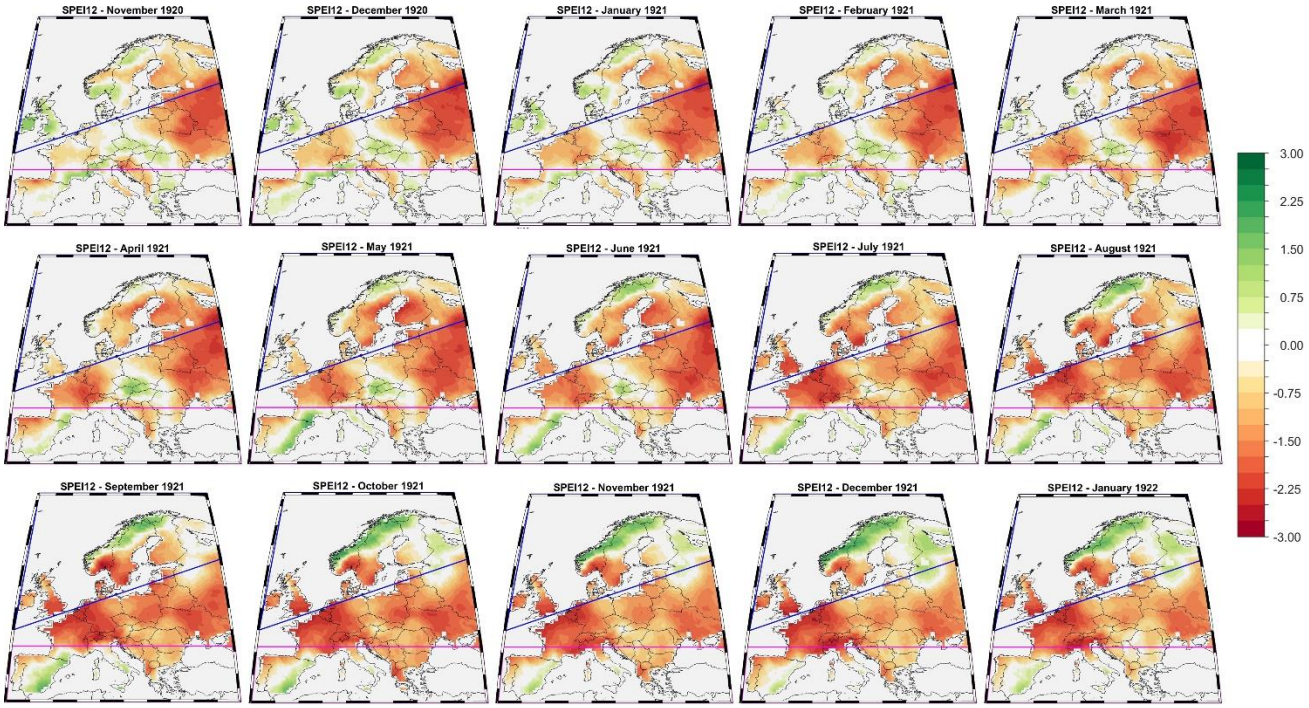

Figure S10. Spatial evolution of the SPEI12 between November 1920 until January 1922.

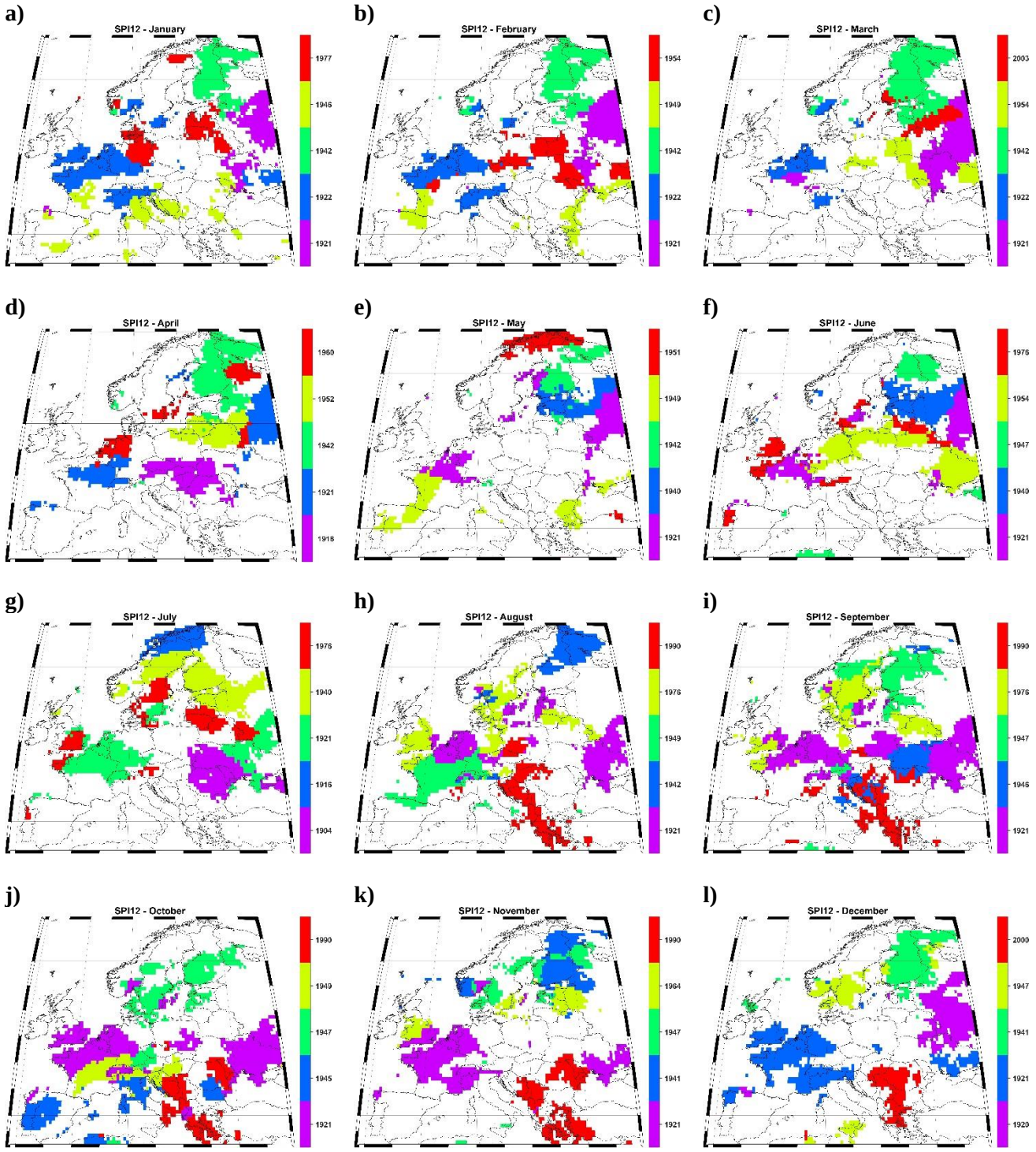

Figure S11. The spatial extent and the year of record of the driest years, based on the monthly SPI12, over Europe. Analyzed period: 1902–2019.

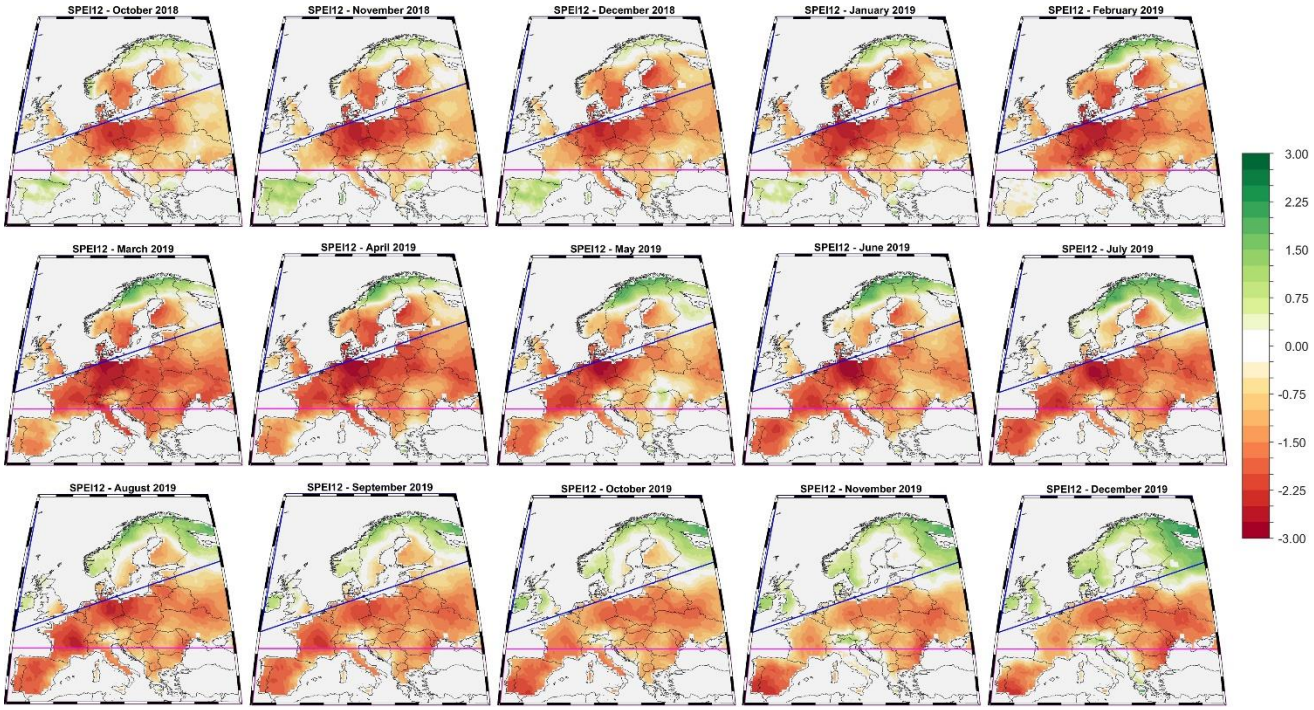

Figure S12. Spatial evolution of the SPEI12 between October 2018 until December 2019.

References

Hamed, K. H. & Rao, A. R. A modified Mann-Kendall trend test for autocorrelated data. *Journal of Hydrology* **204**, 182–196 (1998).

Kendall, M.G., 1948. Rank Correlation Methods. Griffin, London

Mann, H. B., 1945. Nonparametric tests against trend. *Econometrica* **13**, 245–259.

NOAA: ETOPO1 1 Arc-Minute Global Relief Model, Cent. NOAA Natl. Geophys. Data [online] Available from: https://www.ngdc.noaa.gov/mgg/global/ (Accessed 18 October 2020), 2009